Chalcogenide Letters Vol. 11, No. 11, November 2014, p. 597 - 603

EFFECTS OF PREPARATION CONDITIONS ON THE HYDROTHERMAL SYNTHESIS OF $CdIn_2S_4$ POWDER

S. KAOWPHONG[a*], S. KITTIWACHANA[a], N. CHUMHA[a], T. THONGTEM[a], S. THONGTEM[b]

[a]*Department of Chemistry, Faculty of Science, Chiang Mai University, Chiang Mai 50200, Thailand*

[b]*Departments of Physics and Materials Science, Faculty of Science, Chiang Mai University, Chiang Mai 50200, Thailand*

$CdIn_2S_4$ powder was synthesized by a simple hydrothermal method employing L-cysteine as a sulfur source. Effects of pH of the solution, holding time and reaction temperature on purity, crystallinity and microstructure of the products were investigated. The products were characterized by XRD and FTIR, indicating pure $CdIn_2S_4$ with a cubic spinel structure at 240 °C for 48 h with the initial pH (1.8). Based on FESEM and TEM observations, the $CdIn_2S_4$ was an octahedral shape with an average size of 200-250 nm. EDX spectrum showed the existences of Cd, In and S elements with the atomic ratio of 1.00:2.06:3.95. The optical band gap of the $CdIn_2S_4$ was 2.30 eV. It can be seen that pH, holding time and reaction temperature were the important factors for the synthesis of the pure $CdIn_2S_4$ powders. Increase in pH yielded impurity in the products which could be explained by the hard and soft acid base (HSAB) concept. Increase in the length of the holding time could not improve the purity; however, a greater numbers of particles with well-structured octahedrons could be observed. A larger particle sizes with good crystalline structure were provided when high temperatures were used.

(Received October 3, 2014; Accepted November 21, 2014)

Keywords: $CdIn_2S_4$; hydrothermal; octahedron; semiconductor; X-ray diffraction

1. Introduction

Cadmium indium sulfide ($CdIn_2S_4$) is a chalcogenide semiconductor that belongs to the AB_2X_4 family of ternary compounds. This compound has been regarded as a novel visible-light photocatalyst for organic dye degradation [1, 2], photohydrogen production [3] and bacterial inactivation [4]. Moreover, $CdIn_2S_4$ has received much attention due to their potential applications in photoconductors, solar cells, optoelectronic devices and light emitting diodes (LEDs) [5, 6].

$CdIn_2S_4$ was first synthesized through the reaction of CdS, In and S at 800 °C under vacuum condition [7]. It was also prepared by high temperature sintering of CdS and In_2S_3 [8]; however, defects could be generated by non-stoichiometric composition during the high-temperature growth causing poor crystal quality and poor optical transparency [9, 10]. The hydrothermal method was developed as an alternative way to prepare $CdIn_2S_4$ [1, 3, 5, 11, 12]. It is greener than the conventional processes because the reaction is carried out in a closed system at considerably lower temperatures [13, 14]. In addition, this method offers higher diffusivity and lower viscosity therefore better mass transport and higher dissolving power can be achieved. The kinetics of the reactions is also accelerated at the elevated temperatures, leading to the formation of a pure homogeneous and highly crystalline phase [13]. Some of previous hydrothermal reports [1, 3, 5, 11] required thiourea or thioacetamide as a sulfur source, producing pungent hydrogen sulfide [5, 12] that can be harmful to humans and the environment. Therefore, biomolecule-

*Corresponding author: sulawank@gmail.com

assisted synthesis has been applied to prepare the $CdIn_2S_4$ compound. For example, W. Zhang et. al. [15] have reported the deposition of $CdIn_2S_4$ nanosheets thin film on a conductive substrate using L-cysteine as a sulfur source under hydrothermal reactions.

In this research, the $CdIn_2S_4$ powder was hydrothermally prepared with the assistance of L-cysteine, a common amino acid and an environmentally benign sulfur source. Our effort was to investigate the effects of the synthesis conditions such as pH of the solution, holding time and reaction temperature on the purity, microstructure and formation of the $CdIn_2S_4$ powder. The optical band gap of the synthesized powders was also examined.

2. Experimental procedure

2 mmol of $CdCl_2 \cdot 2.5H_2O$ and 4 mmol of $InCl_3 \cdot 4H_2O$ were dissolved in 40 mL of deionized water. Then, 20 mL of 8 mmol L-cysteine was slowly added to the mixture. After stirring for 30 min, the pH of the solution was adjusted by HCl and NaOH. Notably, the initial pH of the mixture solution was 1.8. The solution was again stirred for 30 min. After that, it was transferred into 75 ml lab-made Teflon-lined stainless steel autoclave and maintained at 160°C for 12, 24, 48, 60, and 72 h, respectively. After the reaction system was naturally cooled to room temperature, the yellow precipitate powders were collected, washed several times with de-ionized water and ethanol, respectively, and dried in an oven at 80 °C overnight. The same procedure was repeated by varying reaction temperatures to 200 °C, 240 °C, and 260 °C for 48 h.

Crystallinity and phase purity of the prepared powders were characterized by X-ray diffraction spectroscopy (XRD, Rigaku Miniflex II) with CuKα radiation (λ = 1.5418 Å). Fourier transform infrared spectroscopy (FTIR, Bruker TENSOR27) was used to investigate the vibration modes and residual organic molecules. Particle size and morphology of the products were determined by field emission-scanning electron microscope (FESEM, JEOL JSM-6335F) operated at 15 kV of accelerating voltage and transmission electron microscopy (TEM, JEOL JEM-2010) operating at 200 kV. The chemical composition was analyzed by energy dispersive X-ray spectroscopy (EDX) with an accelerating voltage of 20 kV. UV-Vis spectrum was recorded by UV-Visible spectroscopy (Lamda 25 PerkinElmer, U.S.A.) in the range of 200–800 nm. Optical band gap was estimated by the following equation $\alpha h\nu = (h\nu - E_g)^n$, where α is the absorption coefficient, h is the Planck constant, ν is the photon frequency, E_g is the optical band gap and n is 1/2 for direct-allowed transition [16].

3. Results and discussion

The XRD spectra of the powders prepared at 160^{o}C with different pH are shown in Fig. 1(a). In the highly acidic medium (pH 1 to 3), the XRD signals of CdS was detected (JCPDS Database no. 01-0780) [17]. Once the pH was raised to 5, 7, 9 and 11 by adding NaOH solution, $In(OH)_3$ was detected (JCPDS Database no. 16-0161) [17]. The formation of $In(OH)_3$ was attributed to the reaction between In^{3+} and OH^- ions in the solution. This could be explained by the hard and soft acid base (HSAB) concept [18]. Since In^{3+} is a hard acid and OH^- is a hard base; therefore, a more stable compound formed was $In(OH)_3$ rather than $Cd(OH)_2$. In Fig. 1(a), the XRD spectrum of the powder prepared at the initial pH (1.8) was closely matched with that of cubic structured $CdIn_2S_4$ (JCPDS Database no. 27-0060) [17], although small diffraction signals of CdS appeared in the spectrum. Therefore, the pH of the solutions was kept at the initial pH and the solutions were maintained at 160 ^{o}C for 12, 24, 48, 60, and 72 h, respectively, to investigate the effect of hydrothermal time on the formation of the $CdIn_2S_4$ powders. Fig. 1(b) shows the XRD pattern of the powders prepared at different holding times. The diffraction signals of CdS still appeared in all of the powders. The existence of CdS could be attributable to Cd^{2+} being a soft acid which was more likely to react with a soft base (S^{2-}) than with the hard acid (In^{3+}). Therefore, a greater amount of the CdS compound was produced and remained in the products. The experiment procedure was repeated by varying reaction temperatures to 200 °C, 240 °C, and 260 °C for 48 h

where the pH was kept at 1.8. The XRD pattern of the powders prepared at different reaction temperatures are shown in Fig. 1(c). At 240 °C and 260 °C, no characteristic signals of CdS were detected, indicating that pure $CdIn_2S_4$ powders with a cubic structure were obtained. Strong and sharp diffraction peaks are found, implying that the obtained powders are large crystallite sizes with good crystalline structure. The lattice parameters (a = 10.8325 Å for $CdIn_2S_4$ at 240 °C and a = 10.8306 Å for $CdIn_2S_4$ at 260 °C), calculated using the relationship between Bragg diffraction spacing and cubic cell parameters [18] :

$$d_{hkl} = \frac{a}{\sqrt{h^2 + k^2 + l^2}} \tag{1}$$

where d_{hkl} is the Bragg diffraction spacing for the (hkl) plane, hkl are miller indices and a is a cell parameter. The calculated cell parameters of the powders synthesized under both of the conditions (240 °C and 260 °C) are in accordance with those of the corresponding JCPDS database.

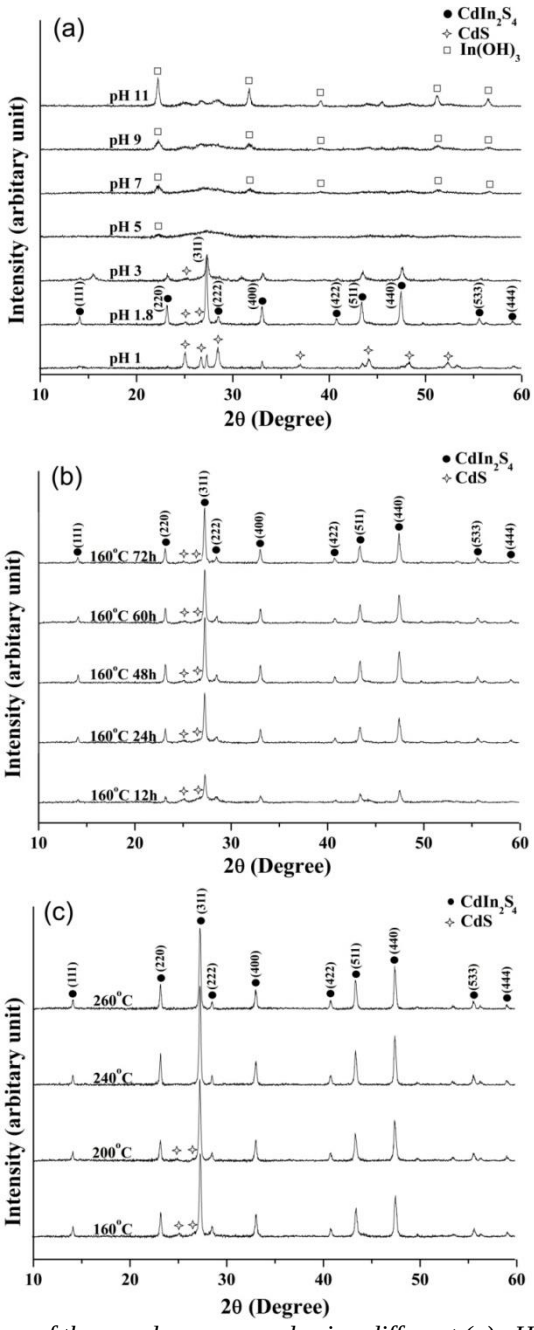

Fig. 1. XRD patterns of the powders prepared using different (a) pH (b) holding times and (c) temperatures.

The FTIR spectra of the powders prepared at 160 °C for 48 h using different pH are shown in Fig. 2(a). When compared with the FTIR spectrum of L-cysteine (Fig. 2(b)), no characteristic absorption peak of S–H group around 2552 cm^{-1} is detected in the FTIR spectra of the powders, demonstrating that the L-cysteine molecules were completely decomposed. Each of the FTIR spectra of the powders prepared at pH 3 to 11 shows a broad band in the range of 3000 to 3700 cm^{-1}, referring to the O–H stretching vibrations in hydroxyl groups and water molecules which are bound by the hydrogen bond [20]. In addition, a weaker band at 1628 cm^{-1} was assigned to the bending vibrations of the O–H groups [20]. The FTIR spectra of the powders prepared at pH 5 to 11 also showed the absorption peaks at 500 cm^{-1} which were assigned to the stretching vibration of In–O bonds [21] and the peaks at 653-853 cm^{-1} and 1066-1160 cm^{-1} were assigned to the stretching and bending vibrations of the In–O–H bonds [21], respectively, which are in good agreement with the XRD results where the diffraction signals of $In(OH)_3$ were indexed.

Fig. 3(a)-(e) show the FESEM images of the $CdIn_2S_4$ powders prepared at different reaction times and temperatures. At 160 °C 12 h (Fig. 3(a)), small flakes assembling in the form of incomplete octahedral-shaped powder were provided. When the reaction time was increased to 48 h (Fig. 3(b)), a greater numbers of particles with well-structured octahedrons and an average diameter of about 150-230 nm could be observed. When the reaction temperatures were increased to 200 °C and 240 °C, the shape of the octahedrons still remained the same as shown in Fig. 3(c) and 3(d), respectively. After the reaction temperature reached 260 °C (Fig. 3(e)), the edge of each of the octahedrons tend to combine through orientation attachment mechanism [22]. In Fig. 3(f), the EDX spectrum of the $CdIn_2S_4$ powder prepared at 240 °C for 48 h with the initial pH presents the existence of Cd, In and S elements. The atomic ratio of Cd, In and S is 1.00:2.06:3.95, illustrating that the stoichiometric ratio of the powder is approximately close to that of $CdIn_2S_4$.

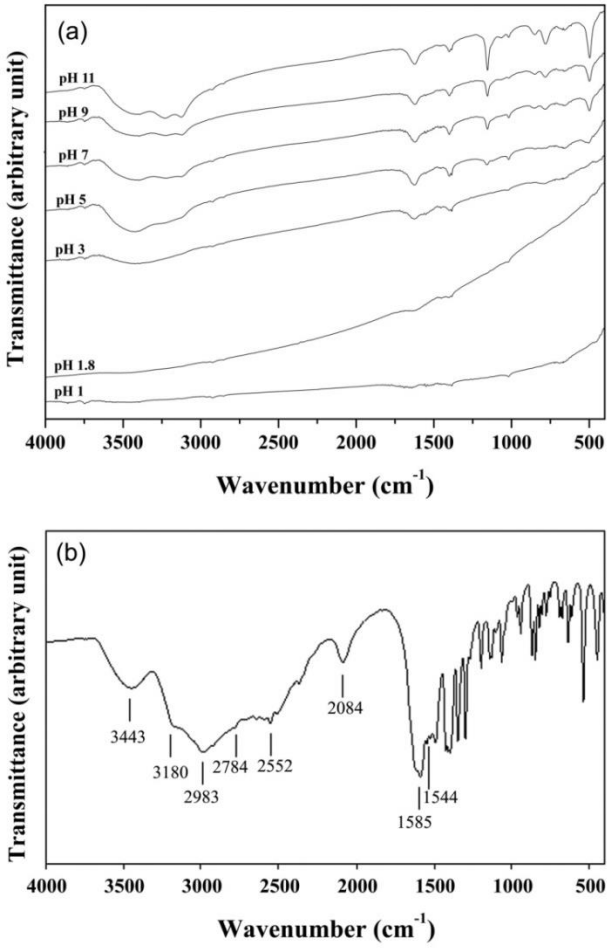

Fig. 2. FTIR spectra of (a) the powders prepared at 160 °C for 48 h using different pH and (b) L-cysteine.

A possible formation mechanism of the$CdIn_2S_4$ powders could be as follows. Owing to the strong ability to coordinate with metal cation as demonstrated by N. Burford et al. [23], L-cysteine molecules reacted initially with Cd^{2+} and In^{3+} to form stable $[Cd(L\text{-cysteine})_n]^{2+}$ and $[In(L\text{-cysteine})_n]^{3+}$ complexes. Upon heating under a given temperature, L-cysteine was attacked by the strong nucleophilic O atoms of H_2O molecules, leading to the weakening of $[Cd(L\text{-cysteine})_n]^{2+}$ and $[In(L\text{-cysteine})_n]^{3+}$ complexes. The C–S bonds in the complexes were gradually broken and then the CdS and In_2S_3 were produced. After that, the CdS and In_2S_3 were combined to form initial $CdIn_2S_4$ particles. The small flakes observed in the SEM image (Fig. 3(a)) could occur from the orientation of the tiny $CdIn_2S_4$ particles. The change from the flake to octahedral shape when the reaction time was prolonged resulted from the self-organization, in accordance with the previous report [1].

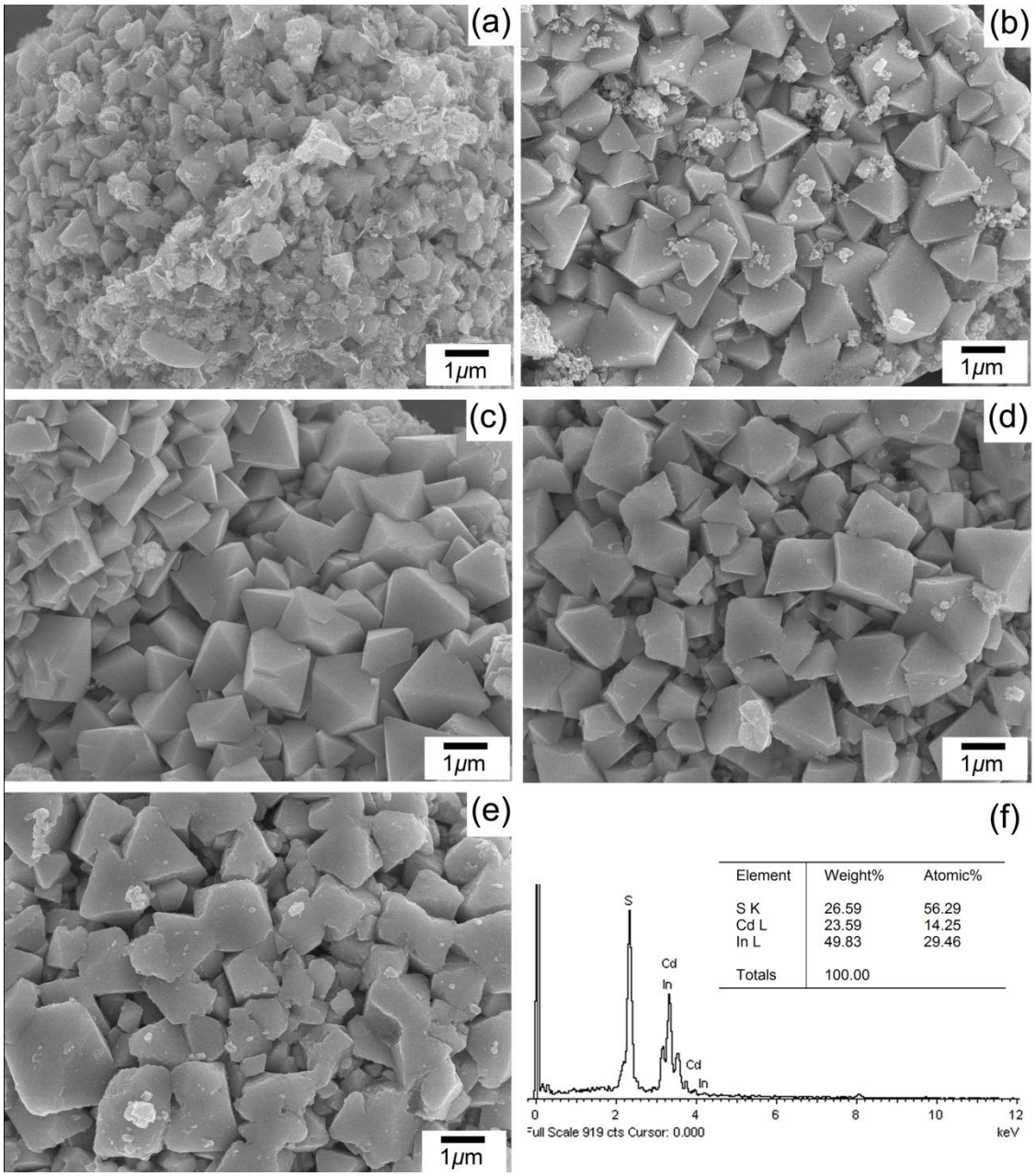

Fig. 3. FESEM images of the $CdIn_2S_4$ powders prepared using the initial pH at (a) 160 °C for 12 h, (b) – (e) 160 °C, 200 °C, 240 °C and 260 °C, respectively, for 48 h and (f) EDX spectrum of the $CdIn_2S_4$ powder prepared at 240 °C for 48 h.

Fig. 4(a) shows the TEM image of the $CdIn_2S_4$ powder prepared at 240 °C for 48 h. It can be seen that the powder is composed of octahedral particles with an average size of about 200 nm. The selected area electron diffraction (SAED) pattern of the $CdIn_2S_4$ octahedron (Fig. 4(b)) was indexed through the $[\bar{1}14]$ electron beam direction. This pattern confirms the cubic structure of the octahedral $CdIn_2S_4$ crystal. High resolution TEM (HRTEM) image showing lattice fringes of the $CdIn_2S_4$ octahedron revealed the crystalline nature of the particles. The spacing between the two adjacent lattice planes was 0.32 nm which corresponded to the (311) plane of cubic structure as shown in Fig. 4(c).

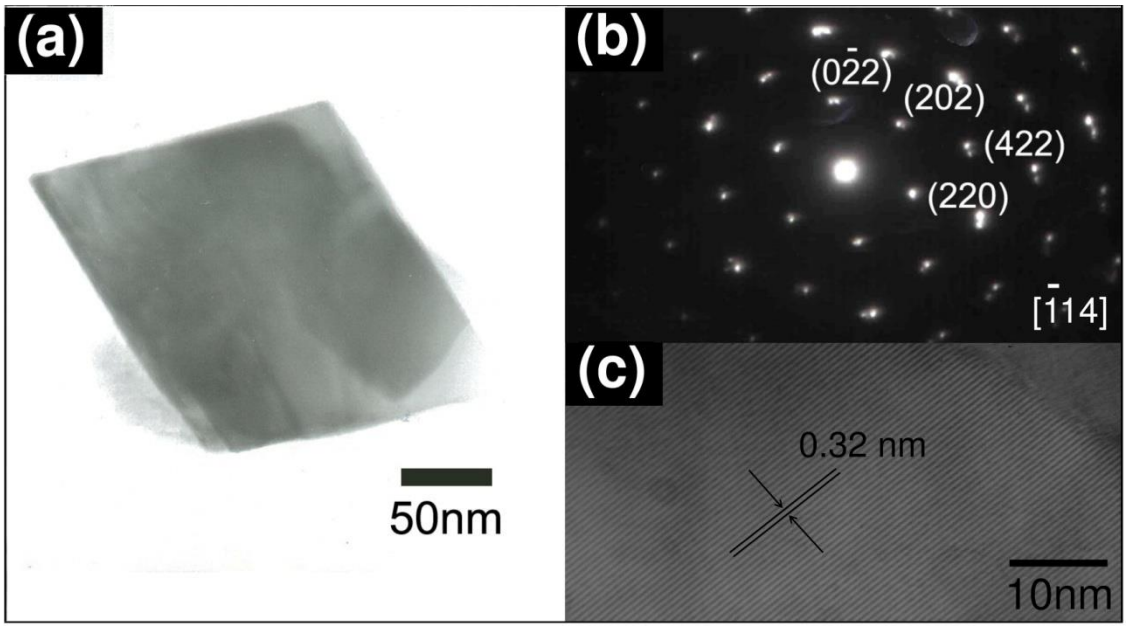

Fig. 4. (a) TEM image, (b) SAED pattern, and (c) HRTEM image of the $CdIn_2S_4$ octahedron prepared at 240 °C for 48 h.

The plot of $(\alpha h\nu)^2$ vs. $h\nu$ of the $CdIn_2S_4$ powder prepared at 240 °C for 48 h is shown in Fig. 5. The value of the optical energy gap was determined by extrapolating the linear portion of the curves to zero absorption ($\alpha = 0$). The estimated direct band gap was 2.30 eV implying the potential applications in photocatalysis due to its narrow band gap that corresponds to visible-light absorption.

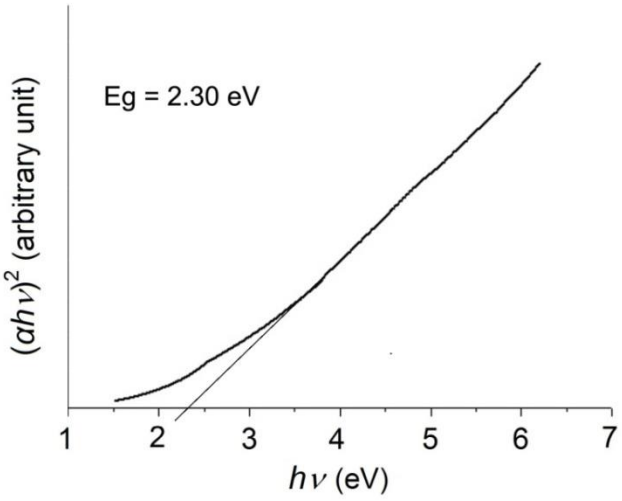

Fig. 5. Plot of $(\alpha h\nu)^2$ vs. $h\nu$ for direct transitions of the $CdIn_2S_4$ powder prepared at 240 °C for 48 h.

4. Conclusions

The $CdIn_2S_4$ powders were synthesized by the hydrothermal route at 240 °C for 48 h. The average size of the $CdIn_2S_4$ octahedrons is 200-250 nm. The pH of the solution and the reaction temperature played an important role in the synthesis of pure $CdIn_2S_4$ powders, whereas the longer holding time could contribute to the increase of particles with well-structured octahedrons.

Acknowledgement

We would like to thank Chiang Mai University for financial support.

References

[1] S. K. Apte, S. N. Garaje, R. D. Bolade, J. D. Ambekar, M. V. Kulkarni, S. D. Naik, S. W. Gosavi, J. O. Baeg, B. B. Kale, J. Mater. Chem. **20**, 6095 (2010).
[2] J. Mu, Q. Wei, P. Yao, X. Zhao, S. Kang, X. Li, J. Alloys Compd. **513**, 506 (2012).
[3] B. B. Kale, J. Baeg, S. M. Lee, H. Chang, S. Moon, C. W. Lee, Adv. Funct. Mater. **16**, 1349 (2006).
[4] W. Wang, T. W. Ng, W. K. Ho, J. Huang, S. Liang, T. An, G. Li, J. C. Yu, P. K. Wong, Appl. Catal. B: Environ. **129**, 482 (2013).
[5] A. Bhirud, N. Chaudhari, L. Nikam, R. Sonawane, K. Patil, J. Baeg, B. Kale, Inter. J. hydrogen energy **36**, 11628 (2011).
[6] R. R. Sawant, K. Y. Rajpure, C. H. Bhosale, Phys. B 393, 249 (2007).
[7] H. Hahn, G. Frank, W. Klingler, A. D. Störger, G. Störger, J. Inorg. Gen. Chem. **279**, 241 (1955).
[8] T. G. Kerimova, E. Y. Salaev, A. S. Khidirov, N. G. Dervishov, S. M. Efendiev, Phys. Status Solidi B **113**, K107 (1982).
[9] S. H. You, K. J. Hong, T. S. Jeong, C. J. Youn, J. S. Park, B. J. Lee, J. W. Jeong, J. Cryst. Growth **271**, 391 (2004).
[10] J. Lu, Y. Xie, G. Du, X. Jiang, L. Zhu, X. Wang, Y.Qian, J. Mater. Chem. **12**, 103 (2002).
[11] L. Fan, R. Guo, J. Phys. Chem. C **112**, 10700 (2008).
[12] J.Q. Hu, B. Deng, W.X. Zhang, K.B. Tang, Y.T. Qian, Inorg. Chem. **40**, 3130 (2001).
[13] M. Yoshimura and K. Byrappa, J. Mater. Sci. **43**, 2085 (2008).
[14] K. Byrappa and T. Adschiri, Prog. Cryst. Growth Charact. Mater. **3**, 117 (2007).
[15] W. Zhang, H. Yang, W. Fu, M. Li, J. Alloys Compd. **561**, 10 (2013).
[16] J. G. Speight, Lange's Handbook of Chemistry, 16th ed, The McGraw-Hill Companies, Inc., New York (2005).
[17] Powder Diffraction File, JCPDS International Centre for Diffraction Data, 12 Campus Boulevard, Newtown Square, PA19073-3273, USA (2001).
[18] J. E. Huheey, E. A. Keiter, R. L. Keiter, Inorganic chemistry: principles of structure and reactivity, 4th ed, Harper Collins College Publishers, New York (2000).
[19] C. Hammond, The Basics of Crystallography and Diffraction, 3rd ed, Oxford University Press, United Kingdom (2009).
[20] D. L. Vien, The Handbook of infrared and raman characteristic frequencies of organic molecules, Academic Press (1991).
[21] M. I. Ivanovskaya, E. A. Ovodok, D. A. Kotsikau, Glass Phy. Chem. **37**, 560 (2011).
[22] J. Zhang, F. Huang, Z. Lin, Nanoscale **2**, 18 (2010).
[23] N. Burford, M. D. Eelman, D. E. Mahony, M. Morash, Chem. Commun. **1**, 146 (2003).